High-order Dy multipole motifs observed in DyB_2C_2 with resonant soft x-ray Bragg diffraction

2006 J. Phys.: Condens. Matter 18 11195

(http://iopscience.iop.org/0953-8984/18/49/012)

INSTITUTE OF PHYSICS PUBLISHING JOURNAL OF PHYSICS: CONDENSED MATTER

J. Phys.: Condens. Matter **18** (2006) 11195–11202 doi:10.1088/0953-8984/18/49/012

High-order Dy multipole motifs observed in DyB_2C_2 with resonant soft x-ray Bragg diffraction

A M Mulders[1], U Staub[1], V Scagnoli[1], S W Lovesey[2,3], E Balcar[4], T Nakamura[5], A Kikkawa[3], G van der Laan[6] and J M Tonnerre[7]

[1] Swiss Light Source, Paul Scherrer Institut, CH 5232 Villigen PSI, Switzerland
[2] ISIS, Rutherford Appleton Laboratory, Chilton, Oxfordshire OX11 0QX, UK
[3] RIKEN SPring-8 Center, Harima Institute, Sayo, Hyogo 679-5148, Japan
[4] Vienna University of Technology, Atominstitut, Stadionallee 2, 1020, Vienna, Austria
[5] SPring-8/JASRI, Mikazuki, Sayo, Hyogo 679-5198, Japan
[6] Daresbury Laboratory, Warrington, Cheshire WA4 4AD, UK
[7] CNRS Grenoble, 38042 Grenoble Cedex 9, France

Received 4 August 2006, in final form 10 October 2006
Published 22 November 2006
Online at stacks.iop.org/JPhysCM/18/11195

Abstract

Resonant soft x-ray Bragg diffraction at the Dy $M_{4,5}$ edges has been exploited to study Dy multipole motifs in DyB_2C_2. Our results are explained by introducing the intra-atomic quadrupolar interaction between the core 3d and valence 4f shell. This allows us to determine for the first time higher-order multipole moments of dysprosium 4f electrons and to draw their precise charge density. The Dy hexadecapole and hexacontatetrapole moment have been estimated at -20% and $+30\%$ of the quadrupolar moment, respectively. No evidence for the lock-in of the orbitals at T_N has been observed, in contrast to earlier suggestions. The multipolar interaction and the structural transition cooperate along c but they compete in the basal plane, explaining the canted structure along [110].

(Some figures in this article are in colour only in the electronic version)

1. Introduction

Resonant x-ray Bragg scattering (RXS) has recently become a powerful tool in modern solid state physics to investigate magnetic, orbital and charge order phenomena associated with electronic degrees of freedom. Especially in transition metal oxides, and, possibly, actinide compounds, various phenomena can occur simultaneously, and it is not easy to identify the exact role and interplay of the various order parameters. However, in rare earth based compounds, orbital and magnetic order occur more autonomously from the lattice as the 4f electrons are shielded by the outer 5d electrons. Electronic orbital motifs are usually labelled antiferroquadrupolar (AFQ) or ferroquadrupolar (FQ), but higher-order multipoles are not established by observations. Argon atoms in an excited state with $l = 3$ show a significant presence of the higher-order multipole moments as concluded from electron scattering [1], but in the solid state multipoles beyond rank 4 have never been detected. Yet the alignment of

higher multipoles to the surrounding charge in the lattice is likely. For 4f electrons ($l = 3$) multipoles up to rank 6 are present, and this results in a undulated and aspheric charge density. Which multipoles dominate these orbital order transitions remains a rather controversial topic, as exemplified in CeB_6 [2], NpO_2 [3] and URu_2Si_2 [4]. Using soft x-ray resonant Bragg scattering (SXRS), we have obtained the first direct evidence of high-order Dy multipole moment motifs in DyB_2C_2.

DyB_2C_2 has attracted much attention lately as its high AFQ ordering temperature $T_Q = 24.7$ K allows one to study this phenomenon conveniently. At room temperature, DyB_2C_2 crystallizes in the tetragonal $P4/mbm$ structure and undergoes a structural transition with small alternating shifts of pairs of B and C atoms along c at T_Q [5] which reduces the symmetry to $P4_2/mnm$ [6]. Below $T_N = 15.3$ K, antiferromagnetic order (AFM) is observed with complex moment orientations due to the underlying orbital interaction [7]. RXS at the Dy L_3 edge has been used to elucidate Dy dipole and quadrupole motifs [6, 8]. A dipole transition (E1) occurs between Dy 2p and 5d shells and a quadrupole transition (E2) between Dy 2p and 4f shells. The first and dominant process probes the quadrupolar order of the 5d states and the latter transition probes the quadrupolar order of the 4f states. The quadrupolar origin of the reflection has been confirmed by azimuthal scans (rotation around the Bragg wavevector).

Ground state wavefunctions of the Dy 4f shell have been proposed based on the observed absence of E2 intensity at the $(00\frac{5}{2})$ charge forbidden reflection which implied cancellation of quadrupole (rank 2) and hexadecapole (rank 4) contributions [9]. These wavefunctions are consistent with a recent inelastic neutron scattering study in which the orbital fluctuation timescale has been determined [10]. An alternative explanation for the RXS data suggests that the hexadecapole moment is zero and that the overlap between the E1 and E2 resonances cancels the E2 intensity [11]. However, the mixing parameter of E1 and E2 processes is fixed at unity in the analysis but this is not *a priori* justified. SXRS at the Dy $M_{4,5}$ edges accesses the 4f shell directly with the E1 transition, *without* the complication of overlapping E1 and E2 resonances. Our results show that the Coulomb (intra-atomic quadrupole) interaction between the 3d and 4f shells is significant. The ordered quadrupole moment of the 4f shell in the intermediate state reshapes the observed $3d_{5/2}$ and $3d_{3/2}$ core hole charge density and leads to a core hole splitting. It is shown that this phenomenon causes interference between different pathways of the scattering amplitude, allowing the extraction of high-order multipole moments of the 4f shell that have rank 4 and rank 6 (hexacontatetrapole).

2. Experimental details

A DyB_2C_2 single crystal was grown by the Czochralski method using an arc-furnace with four electrodes and cut with (001) perpendicular to the sample surface. Subsequently, it was polished and aligned with 26°, 56° or 86° azimuthal angle. Zero degree azimuth corresponds to alignment of the b axis in the scattering plane. The orbital ordering $(00\frac{1}{2})$ reflection was recorded at the Dy $M_{4,5}$ edges of DyB_2C_2 at the RESOXS end-station of the SIM beam-line at the Swiss Light Source. The Dy $M_{4,5}$ absorption edges were characterized with fluorescence yield (FY) and electron yield (EY) at RESOXS and the BL25SU beam line at SPring-8, respectively.

3. Results

3.1. Resonant x-ray diffraction

The recorded energy profile of the charge-forbidden $(00\frac{1}{2})$ reflection of DyB_2C_2 is shown in figure 1(b), together with x-ray absorption (XAS) data (EY) (figure 1(a)). We note that the

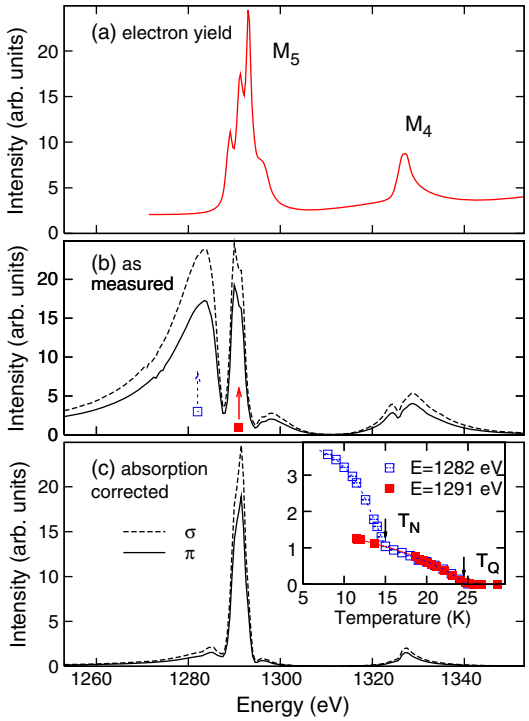

Figure 1. (a) Absorption of DyB_2C_2 recorded in electron yield, (b) diffraction intensity of orbital ordering $(00\frac{1}{2})$ reflection in DyB_2C_2 taken with incident σ and π polarization at $T = 18$ K and (c) diffracted intensity of (b) corrected for absorption effects. The inset shows the intensity as a function of temperature for $E = 1282$ and 1291 eV normalized to 1 at T_N for easy comparison.

diffracted intensity was recorded with a photodiode and the read-out noise results in errors smaller than the point size of the plots in this paper. Multiple features are observed with much larger energy spread than the multiplet structure of the XAS data, in contrast with the single oscillator recorded at the Dy L_3 edge [9]. A similar energy profile has been reported for the M_5 edge of Ho at the magnetic $(0, 0, \tau)$ reflection but the central sharp feature (solid symbol in figure 1) is absent [12]. The authors argue that the large photo-absorption causes this 'gap' at the M_5 edge because strong absorption is inherent to soft x-ray scattering. To characterize the width of the scattering $\theta/2\theta$-scans were recorded for the $(00\frac{1}{2})$ reflection at each energy. Subsequently, the integrated intensity was corrected for absorption, and the corrected curve is shown in the figure 1(c). Absorption effects hugely reduce the intensity of the central feature but cannot account for the multiple features in the energy dependent intensity. The different character of those structures becomes even more apparent from the temperature dependence of the scattered intensity. The AFM transition is witnessed at 15 K as a gradual increase in intensity at 1282 eV; however, this increase is absent at 1291 eV (see inset of figure 1). This cannot be caused by absorption effects on a single oscillator resonance. It appears that the scattered intensity at 1291 eV is sensitive to the orbital order only and its gradual increase below T_N shows that there is no lock-in of the orbitals as proposed from neutron diffraction and symmetry analysis [13]. We will return to this point in the discussion.

The structure in the energy profile is similar for σ and π polarization of the incident x-rays and independent of the sample temperature in the AFQ phase. Azimuthal angles of 56° and 86° give the same spectral shape but show different overall intensity, as expected from the

azimuthal angle dependence of a quadrupole. This illustrates that one atomic tensor is active in the scattering process.

We propose that this particular shape of the energy dependence of the $(00\frac{1}{2})$ reflection is caused by the splitting of the 3d core states which results in multiple interfering resonators and consequently adds structure to the energy profile. Previously a core hole splitting caused by the intra-atomic magnetic interaction between 5f and 3d was used to describe the unusual double Lorentzian energy profile at the M_4 resonance in NpO_2 [14]. There is no ordered magnetism in the AFQ phase and we introduce the intra-atomic *quadrupolar* interaction to partially lift the core hole degeneracy. The energy splitting is determined by the strength of the intra-atomic interaction and we show that the relative amplitudes are determined by the 4f wavefunction. Thus, the spectral shape is constant in the AFQ phase. Note that the diffracted intensity is caused by the bulk order and is subject to critical fluctuations while the energy splitting is due to the local orbital moment of the 4f shell and is independent of its orientation.

In section 3.2 we will first encapsulate the resonant diffraction theory specific to our problem and introduce the intra-atomic quadrupole interaction to portray the observed energy dependence.

3.2. Theoretical framework

The scattered photon intensity $\mathrm{d}\sigma/\mathrm{d}\Omega$ is proportional to the squared modulus of the amplitude f [15]

$$f = \sum_{K,Q} (2K+1)^{\frac{1}{2}} X^K_{-Q} \sum_q D^K_{Qq}(\alpha,\beta,\gamma) F^K_q, \tag{1}$$

which is described as a product of spherical tensors with rank K. F^K_q with $-K \leqslant q \leqslant K$ describes the electronic response of the sample. X^K_{-Q} with $-K \leqslant Q \leqslant K$ describes the geometry of the experimental set-up and polarization direction of the incident and reflected x-rays. Lastly, $D^K_{Qq}(\alpha,\beta,\gamma)$ rotates F^K_q onto the coordinates of the experimental reference frame used for X^K_{-Q} with Euler angles α, β, γ. The Dy site symmetry of $2/m$ gives $q = \pm 2$ and $K = 2$ due to the absence of charge ($K = 0$) and time-odd (magnetic) ($K = 1$) order at $(00\frac{1}{2})$ in the AFQ phase.

F^K_q describes the atomic resonant process which is commonly represented by a harmonic oscillator. In our particular case we extend the existing theory so that F^K_q is a sum of several oscillators at the E1 resonance created by the splitting of the core state. The amplitude $A^K_q(\bar{J},\bar{M})$ of each oscillator is labelled by the total angular momentum $\bar{J} = \frac{3}{2}, \frac{5}{2}$ and magnetic quantum number $\bar{M}$ of the core hole.

$$F^K_q \propto \sum_{\bar{J},\bar{M}} \frac{r_{\bar{J}} A^K_q(\bar{J},\bar{M})}{E - \Delta_{\bar{J}} - \epsilon(\bar{J},\bar{M}) + \mathrm{i}\Gamma_{\bar{J},\bar{M}}}. \tag{2}$$

Here, E is the photon energy, $\Delta_{\bar{J}}$ is the difference in energy between the degenerate $3d_{\bar{J}}$ shell and the 4f empty states and $\Gamma_{\bar{J},\bar{M}}$ the lifetime of the intermediate state. $\epsilon(\bar{J},\bar{M}) = [3\bar{M}^2 - \bar{J}(\bar{J}+1)]Q_{\bar{J}}$ is the energy shift of the 3d core levels due to the intra-atomic quadrupole interaction $Q_{\bar{J}}$, similar to that in Mössbauer spectroscopy. $Q_{\bar{J}}$ is a product of the 3d quadrupole moment and the f-electron electric field gradient experienced by the 3d electrons with $Q_{\pm\frac{3}{2}}/Q_{\pm\frac{5}{2}} = 7/3$.

There are three resonant oscillators at the M_5 edge ($\bar{M} = \pm\frac{5}{2}, \pm\frac{3}{2}, \pm\frac{1}{2}$) and two at the M_4 edge ($\bar{M} = \pm\frac{3}{2}, \pm\frac{1}{2}$). The amplitudes interfere and the branching ratio between the two edges is defined as a real mixing parameter $r_{\bar{J}}$. $A^K_q(\bar{J},\bar{M})$ is constructed from the structure factor of

Table 1. Reduced matrix elements $R^K(r, x)$ for $K = 2$.

	$\bar{J} = \frac{3}{2}$		$\bar{J} = \frac{5}{2}$		
x	2	4	2	4	6
$r = 0$	$-\frac{2}{21}\sqrt{\frac{34}{35}}$	0	$-\frac{2}{21}\sqrt{\frac{17}{105}}$	0	0
2	$\frac{4}{735}\sqrt{17}$	$\frac{36}{1225}\sqrt{\frac{969}{65}}$	$-\frac{2}{735}\sqrt{\frac{17}{21}}$	$\frac{66}{1225}\sqrt{\frac{323}{455}}$	0
4	0	0	$\frac{2}{147}\sqrt{\frac{17}{35}}$	$-\frac{2}{735}\sqrt{\frac{646}{3003}}$	$-\frac{1}{15}\sqrt{\frac{646}{385}}$

the chemical unit cell Ψ_q^x:

$$A_q^K(\bar{J}, \bar{M}) = (-1)^{\bar{J}-\bar{M}} \sum_r (2r+1) \begin{pmatrix} \bar{J} & r & \bar{J} \\ -\bar{M} & 0 & \bar{M} \end{pmatrix} \sum_x \begin{pmatrix} K & r & x \\ -q & 0 & q \end{pmatrix} R^K(r, x) \Psi_q^x, \quad (3)$$

where $R^K(r, x)$ are reduced matrix elements, $r = 0, 1, \ldots, 2\bar{J}$, $x = |K - r|, \ldots, |K + r|$ and $q + x$ and $r + x$ are both even integers. The relevant reduced matrix elements $R^K(r, x)$ are listed in table 1.

The Dy site symmetry, $2/m$, dictates further that $A_2^2 = -A_{-2}^2$ and

$$\Psi_q^x = \sum_{\mathbf{d}} e^{i\tau\mathbf{d}} \langle T_q^x \rangle_{\mathbf{d}} = 2\{\langle T_q^x \rangle - \langle T_{-q}^x \rangle\} \quad (4)$$

$$\langle T_q^x \rangle = \langle \varphi_0 | T_q^x | \varphi_0 \rangle. \quad (5)$$

T_q^x is the atomic spherical tensor of the Dy 4f shell and $|\varphi_0\rangle$ its ground state wavefunction. It follows that $A_q^K(\frac{5}{2}, \bar{M})$ contains the hexadecapole moment $\langle T_2^4 \rangle$ and hexacontatetrapole moment $\langle T_2^6 \rangle$ in addition to the quadrupole moment $\langle T_2^2 \rangle$. In the case $\epsilon(\bar{J}, \bar{M}) = 0$ the terms proportional to $\langle T_2^4 \rangle$ and $\langle T_2^6 \rangle$ cancel and $A_q^K(\bar{J})$ is proportional to $\langle T_2^2 \rangle$ as usual. This allows one to measure the ordered hexacontatetrapole moment of an electronic shell in solid state physics. The azimuthal angle dependence follows from $D_{Qq}^K(\alpha, \beta, \gamma)$ (equation (1)) and is independent of the relative oscillator strengths, resulting in a spectral shape that is independent of the azimuthal angle.

Let us here summarize the consequences of this analysis of the scattering. The overall intensity is represented by scattering from the quadrupole $\langle T_2^2 \rangle$ of the 4f shell and reflects the same azimuthal angle dependence as the quantity observed in the dipole transition at the L_3 edge [9]. The dependence on the higher 4f multipoles arises from the splitting of the core hole states, which results in the $\bar{M}$ dependence of the amplitudes of the different harmonic oscillators (equation (2)). Correspondingly, these amplitudes are influenced by higher 4f multipoles as shown in equation (3). Therefore, the core hole splitting allows one, for the first time, to measure the ordered hexacontatetrapole moment of an electronic shell in solid state physics. Note that this is not in contradiction with the fact that the integrated intensity of a dipole (E1) transition is sensitive to tensors up to rank 2 (quadrupole), while a quadrupole (E2) transition is sensitive to tensors up to rank 4 (hexadecapole).

4. Discussion

Figure 2 shows the measured energy dependence compared to the above theory. The absorption correction is implemented in the theoretical description for easier visual comparison of the

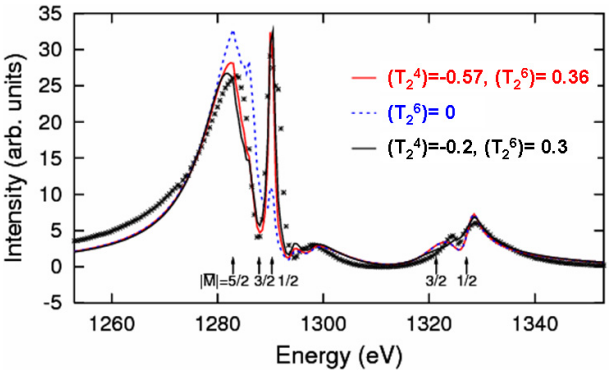

Figure 2. Observed energy profile (crosses) compared to fits of the theory including absorption correction with (a) wavefunction taken from [9] (grey (red)), (b) $\langle T_2^6 \rangle$ set to zero (dotted grey (blue)), and (c) $\langle T_2^x \rangle$ as free parameter (black). $\langle T_2^2 \rangle$ is normalized to 1, $\langle T_2^4 \rangle = -0.2$, $\langle T_2^6 \rangle = +0.3$, $\Gamma_{\frac{5}{2},\pm\frac{1}{2}} = 0.8$ eV, $\Gamma_{\frac{5}{2},\pm\frac{3}{2}} = 2.7$ eV, $\Gamma_{\frac{5}{2},\pm\frac{5}{2}} = 5.3$ eV, $\Gamma_{\frac{3}{2},\pm\frac{1}{2}} = 1.9$ eV and $\Gamma_{\frac{3}{2},\pm\frac{3}{2}} = 5.4$ eV, $r_{\frac{3}{2}} = 0.22$ and $Q_{\frac{5}{2}} = -0.41$ eV.

experimental data and fit. $\Delta_{\bar{J}}$ typically depicts the onset of an absorption edge and $r_{\frac{3}{2}}$ is calculated and reference [16] calculates $r_{3/2} = 0.22$ which is in excellent agreement with our SXRS data. $Q_{\frac{5}{2}} = -0.4$ eV and the resonance positions are indicated in figure 2. The linewidth increases progressively from 0.8 eV for $\bar{M} = \pm\frac{1}{2}$ to 5.3 eV for $\bar{M} = \pm\frac{5}{2}$. $|A_q^K(\frac{5}{2}, \pm\frac{3}{2})|$ is relatively small. The fit results for $r_{\frac{3}{2}}$ and $Q_{\frac{5}{2}}$ turn out to be largely independent of choice of wavefunction and linewidths, but variations in $\langle T_2^x \rangle$ can be partially compensated by the line widths to yield a similar result. The best fit gives $\langle T_2^4 \rangle = -0.2$ and $\langle T_2^6 \rangle = 0.3$. The 4f ground state wavefunction taken from [9] corresponds to $\langle T_2^4 \rangle = -0.57$ and $\langle T_2^6 \rangle = 0.36$ and a fit with these parameters fixed and otherwise free parameters also describes the data well. Both fits as well as the effect of setting $\langle T_2^6 \rangle$ to zero are shown in figure 2.[8] The temperature dependence observed at 1282 and 1291 eV supports our analysis since the resonant cross section contains additional time odd terms due to the magnetic order below T_N. These terms may add at $\epsilon(\frac{5}{2}, \pm\frac{5}{2})$ while they cancel at $\epsilon(\frac{5}{2}, \pm\frac{1}{2})$. In addition our analysis predicts a spectral shape independent of azimuthal angle, consistent with our observation.

The Dy 4f charge density obtained from the best fit is illustrated in figure 3. It supports a 90° zig-zag alignment along c as demonstrated by its protrusions at top and bottom. In the basal plane a 90° zig-zag alignment along [110] is preferred so that the concave part points toward the convex part of its nearest neighbour. Yet, the absence of lock-in of the orbitals confirm that the orbital motif in the AFQ phase is similar to that in the combined AFQ and AFM phase. Therefore the Dy charge densities are canted away from [110] as determined by neutron diffraction [7]. Canted charge densities in the AFQ phase are in agreement with RXS studies [5, 6]. In contrast, Zaharko *et al* [13] argue that a 90° arrangement of neighbouring quadrupoles in the xy plane is most likely because the AFM interaction is not strong enough above T_N to oppose the arrangement favoured by the AFQ interaction. However, such a canted AFQ structure logically emerges when the pairwise movement of B and C ions is in competition with the multipolar interaction and promotes parallel alignment of the orbitals along [110].[9] In contrast, the 90° zig-zag alignment along c is supported by both mechanisms. This is consistent

[8] Note that the reduced matrix elements are contained in equation (3) while in [9] they are included in $\langle T_2^x \rangle$.
[9] See figure 4b of [13] for specific movement of B and C.

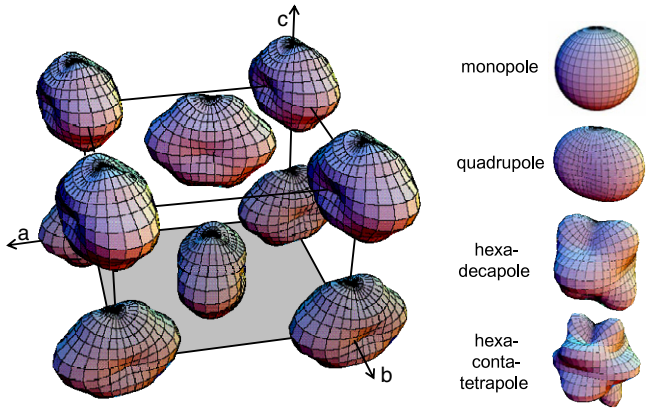

Figure 3. Dy charge density and multipole motif in the AFQ phase of DyB_2C_2. The basal plane is indicated in grey. Note the 90° zig-zag alignment of the Dy orbitals along c and the canted zig-zag alignment along [110]. A spherical charge density has been subtracted to emphasize the asphericity.

with a recent study of (Dy, Y)B_2C_2 where quasi-one-dimensional AFQ along the c axis has been reported [17].

We should add that our analysis in terms of core–valence interaction is consistent with the multiplet structure interpretation. In the M_5 and M_4 absorption the multiplet structure is ∼10 eV and ∼5 eV wide, respectively, which is mainly due to the strong 3d–4f and 4f–4f Coulomb and exchange interactions [16]. The $3d^9_{5/2}4f^{10}$ and $3d^9_{3/2}4f^{10}$ final state multiplets contain 6006 and 4004 levels with an average lifetime width of 0.27 and 0.55 eV, respectively. The strong electron correlation leads to non-diagonal matrix elements in the quantum numbers $\bar{L}\bar{S}\bar{J}$ of the core hole. The levels of the same $\bar{M}$ connected by these non-diagonal elements excite partly coherently. This makes it difficult to separate the core hole states. In the free ion we do not expect an energy shift for distributions of different $|\bar{M}|$. This was confirmed for the x-ray absorption spectrum with Cowan's atomic Hartree–Fock code, where we found roughly an equally broad multiplet when switching off the quadrupole component of the orbital contribution of the core–valence interaction. This suggests that any energy shifts in the $|\bar{M}|$ distributions will be due to multipolar ordering of the 4f states.

In this theoretical framework the core hole state is uncoupled from the $4f^{n+1}$ state and the effect of the 4f multiplet structure is indirectly taken into account by the effective widths of the $\bar{M}$ distributions, which exceed the intrinsic life time width and describe the data surprisingly well. Our work merely demonstrates that including the intra-atomic interaction is a viable approach and accounts for the multiple spectral features and their broad distribution in energy. We note that the empty states of the 4f shell selected by the resonant diffraction process, and their corresponding relative transition intensities, are not necessarily the same as for the absorption process. Resonant diffraction is sensitive to the difference between electronic states while absorption spectroscopy is sensitive to its average. For example, the magnetic moment of an antiferromagnet is not visible at the absorption edge, but resonant diffraction may yield large intensities proportional to the magnetic moment [18].

5. Conclusion

In conclusion, the Dy 4f hexadecapole and hexacontatetrapole moments in DyB_2C_2 have been measured with SXRS and their magnitudes are determined at −20% and +30% of the

quadrupole moment, respectively. The orbital order remains unaffected by magnetic order below T_N and no lock-in of the orbitals takes place, in contrast to CeB_6. The structural transition and multipolar interactions cooperate along the *c* axis while they compete along [110]. These findings amply demonstrate a new extension of the resonant x-ray Bragg diffraction method for the observation of high-order electronic multipole motifs. Of particular interest are materials in which higher-order multipoles are believed to be of importance, such as CeB_6, URu_2Si_2, as well as the RB_2C_2 and skutterudite families.

Acknowledgments

We thank O Zaharko for valuable discussion. This work was supported by the Swiss National Science Foundation and performed at the SLS of the Paul Scherrer Institute, Villigen PSI, Switzerland.

References

[1] Al-Khateeb H M, Birdsey B G and Gay T J 2000 *Phys. Rev. Lett.* **85** 4040
[2] Plakhty V P, Regnault L P, Goltsev A V, Gavrilov S V, Yakhou F, Flouquet J, Vettier C and Kunii S 2005 *Phys. Rev.* B **71** 100407
[3] Kubo K and Hotta T 2005 *Phys. Rev.* B **71** 140404(R)
[4] Kiss A and Fazekas P 2005 *Phys. Rev.* B **71** 054415
[5] Adachi H, Kawata H, Mizumaki M, Akao T, Sato M, Ikeda N, Yanaka Y and Miwa H 2002 *Phys. Rev. Lett.* **89** 206401
[6] Tanaka Y, Inami T, Nakamura T, Yamauchi H, Onodera H, Ohoyama K and Yamaguchi Y 1999 *J. Phys.: Condens. Matter* **11** L505
[7] Yamauchi H, Onodera H, Ohoyama K, Onimaru T, Kosaka M, Ohashi M and Yamaguchi Y 1999 *J. Phys. Soc. Japan* **68** 2057
[8] Hirota K, Oumi N, Matsumura T, Nakao H, Wakabayashi Y, Murakami Y and Endoh Y 2000 *Phys. Rev. Lett.* **84** 2706
[9] Tanaka Y, Inami T, Lovesey S W, Knight K S, Yakhou F, Mannix D, Kokubun J, Kanazawa M, Ishida K, Nanao S, Nakamura T, Yamauchi H, Onodera H, Ohoyama K and Yamaguchi Y 2004 *Phys. Rev.* B **69** 024417
[10] Staub U, Mulders A M, Zaharko O, Janssen S, Nakamura T and Lovesey S W 2005 *Phys. Rev. Lett.* **94** 036408
[11] Matsumura T, Okuyama D, Oumi N, Hirota K, Nakao H, Murakami Y and Wakabayashi Y 2005 *Phys. Rev.* B **71** 012405
[12] Spencer P D, Wilkins S B, Hatton P D, Brown S D, Hase T P A, Purton J A and Fort D 2005 *J. Phys.: Condens. Matter* **17** 1725
[13] Zaharko O, Sikora W, Bialas F, Staub U and Nakamura T 2004 *Phys. Rev.* B **69** 224417
[14] Lovesey S W, Balcar E, Detlefs C, van der Laan G, Sivia D S and Staub U 2003 *J. Phys.: Condens. Matter* **15** 4511
[15] Lovesey S W, Balcar E, Knight K S and Fernández-Rodríguez J 2005 *Phys. Rep.* **411** 233
[16] Thole B T, van der Laan G, Fuggle J C, Sawatzky G A, Karnatak R C and Esteva J M 1985 *Phys. Rev.* B **32** 5107
[17] Indoh K, Tobo A, Ohoyama K and Onodera H 2004 *J. Phys. Soc. Japan* **73** 1554
[18] Lovesey S W and Collins S P 1996 *X-ray Scattering and Absorption by Magnetic Materials* (Oxford: Clarendon)